

APPLICATION OF DEEP QUANTUM NEURAL NETWORKS TO FINANCE

TAKAYUKI SAKUMA

ABSTRACT. Use of the deep quantum neural network proposed by Beer et al. (2020) could grant new perspectives on solving numerical problems arising in the field of finance. We discuss this potential in the context of simple experiments such as learning implied volatilities and differential machine proposed by Huge and Savine (2020). The deep quantum neural network is considered to be a promising candidate for developing highly powerful methods in finance.

1. INTRODUCTION

Recently, the rapid development of quantum computing has been eye-opening, and the use of quantum computers in daily life is expected in the near future. The great potential of quantum computing in the financial industry has been actively investigated. An amplitude estimation algorithm was proposed by Brassard et al. (2002) for use in the quantum Monte Carlo method, and Woerner and Egger (2019) applied the algorithm to valuation of Value at Risk (VaR) and Conditional Value at Risk (C-VaR) to achieve quadratic convergence. The amplitude estimation has also been applied by Ramos-Calderer et al. (2019) for an asset probability distribution mapped to unary representation. Additionally, in Fontanela et al. (2019), the original partial differential equation satisfied by the option price is transformed to a Schrödinger equation in imaginary time and the equation is then solved numerically using a hybrid algorithm, where both classical and quantum computing are used.

In this paper, we discuss the potential of applying the deep quantum neural network (DQNN) proposed by Beer et al. (2020) to the field of finance. The DQNN avoids the problem of "barren plateaus" found by McClean et al. (2018) and shows some degree of robustness to noise, which is a major issue in noisy intermediate-scale quantum devices (NISQs). Application of the DQNN to finance is very promising because deep learning has been shown to be efficient for solving high-dimensional problems, including those arising in finance (for example, Gnoatto et al. (2020)). One remarkable feature of quantum computing that attracts researchers is the basic bit, called a qubit. A qubit can utilize the superposition property of a quantum state to express an arbitrary state between 0 and 1 at the same time, while classical bits can only express 0 or 1. Therefore, the use of the DQNN in finance is a natural next step to discovering highly efficient methods for solving numerical problems. We discuss this potential in the context of simple experiments such as learning implied volatilities and differential machine learning proposed by Huge and Savine (2020).

2. DEEP QUANTUM NEURAL NETWORKS

Here, we give a brief explanation of the DQNN proposed by Beer et al. (2020). The scheme is a natural generalization of a conventional neural network, and succeeds in avoiding the issue of the "barren plateau" discovered by McClean et al. (2018), which arises in quantum neural networks (QNNs) but not in conventional neural networks. Let us consider N training pairs $(|\phi_n^{in}\rangle, |\phi_n^{out}\rangle)$ ($n = 1, \dots, N$). Both the input $|\phi_n^{in}\rangle$ and output $|\phi_n^{out}\rangle$ represent some quantum state that satisfies the following relation:

$$(2.1) \quad |\phi_n^{out}\rangle = U|\phi_n^{in}\rangle,$$

where U is an unknown unitary operator. The DQNN is composed of an input layer, an output layer, and L hidden layers. The output is given as the density matrix $\rho_n^{out} = |\phi_n^{out}\rangle\langle\phi_n^{out}|$, where

$$(2.2) \quad \rho_n^{out} \equiv tr_{in, hid}(\mathcal{U}(\rho_n^{in} \otimes |0\dots 0\rangle_{hid, out}\langle 0\dots 0|)\mathcal{U}^\dagger)$$

Date: October 1, 2021.

Key words and phrases. option pricing, neural networks, quantum machine learning, differential machine learning.
Faculty of Economics, Soka University. e-mail: tsakuma@soka.ac.jp.

and $\mathcal{U} \equiv U^{out}U^L U^{L-1} \dots U^1$. Here, U^l represents a unitary layer acting as a perceptron on the qubits in layer l and layer $l-1$. The first key property of the DQNN is that ρ_n^{out} can be expressed as a sequence of layer-to-layer channels ε^l :

$$(2.3) \quad \rho_n^{out} = \varepsilon^{out}(\varepsilon^L(\dots(\varepsilon^2(\varepsilon^1(\rho_n^{in}))))\dots),$$

where

$$(2.4) \quad \varepsilon^l(X^{l-1}) \equiv tr_{l-1}(\prod_{j=m_l}^l U_j^l(X^{l-1} \otimes |0\dots 0\rangle_l \langle 0\dots 0|) \prod_{j=1}^{m_l} \mathcal{U}_j^{l\dagger}).$$

Here, m_l is the number of perceptrons acting on layers l and $l-1$, and U_j^l is the j th perceptron acting on layers l and $l-1$. This expression implies that the information from the input flows from layer to layer, which can be regarded as an equivalent expression of the backpropagation algorithm utilized in conventional neural networks. The cost function C is defined as

$$(2.5) \quad C \equiv \frac{1}{N} \sum_{n=1}^N \langle \phi_n^{out} | \rho_n^{out} | \phi_n^{out} \rangle$$

and varies between 0 and 1. This form reflects the idea of fidelity, which represents how close the output state is to the training state. C takes a value of 1 if the output state is identical to the training state, and the network is thus updated as follows so that C approaches 1:

$$(2.6) \quad U \rightarrow e^{iK\epsilon}U,$$

where K represents the parameterized matrix chosen such that C increases the most rapidly. That is, K is determined such that it maximizes ΔC :

$$(2.7) \quad \Delta C = \frac{\epsilon}{N} \sum_{n=1}^N tr((\sigma_n^l)(\Delta \varepsilon^l)(\rho_n^{l-1})),$$

where ϵ is the step size, $\rho_n^l = \varepsilon^l(\dots(\varepsilon^2(\varepsilon^1(\rho_n^{in}))))\dots$, $\sigma_n^l = \mathcal{F}^{l+1}(\dots \mathcal{F}^{out}(|\phi_n^{out}\rangle \langle \phi_n^{out}|)\dots)$, and \mathcal{F} is the adjoint channel of ε . Then, element of K is represented as follows:

$$(2.8) \quad K_j^l = \eta \frac{2^{m_l-1}}{N} \sum_{n=1}^N tr_{rest} M_j^l,$$

where

$$(2.9) \quad M_j^l = [\prod_{\alpha=j}^1 U_\alpha^l(\rho_n^{l-1} \otimes |0\dots 0\rangle_l \langle 0\dots 0|) \prod_{\alpha=1}^j U_\alpha^{l\dagger}, \prod_{\alpha=j+1}^{m_l} U_\alpha^{l\dagger}(\mathbb{I}_{l-1} \otimes \sigma_n^l) \prod_{\alpha=m_l}^{j+1} U_\alpha^l].$$

rest in (2.8) denotes the complement of α , and η is the learning rate. The second remarkable property of the DQNN is that in order to evaluate K_j^l , only the output of the previous layer, ρ_n^{l-1} , which is obtained using feedforward, and the state of the following layer, σ_n^l , are needed. This helps reduce the memory requirement for executing the DQNN. The trade-off here is that multiple evaluations of the network are needed, but this is not an obstacle for NISQs.

3. LEARNING IMPLIED VOLATILITIES AS AN APPLICATION TO FINANCE

In order to use financial data in the DQNN, we first need to convert the data to qubits. As a simple demonstration, we consider the learning of implied volatilities in the option market: the input data is the strike K_1, K_2, \dots, K_N and the output data is the corresponding implied volatility $\sigma_{imp, K_1}, \sigma_{imp, K_2}, \dots, \sigma_{imp, K_N}$. These data are converted to the following quantum states for $n = 1, 2, \dots, N$:

$$(3.1) \quad |\phi_n^{in}\rangle = \cos\left(\frac{1}{1 + \exp(-(\frac{F}{K_n})^\beta)} \cdot \frac{\pi}{2}\right)|0\rangle + \sin\left(\frac{1}{1 + \exp(-(\frac{F}{K_n})^\beta)} \cdot \frac{\pi}{2}\right)|1\rangle,$$

$$(3.2) \quad |\phi_n^{out}\rangle = \cos\left(\frac{1}{1 + \exp(-(\frac{\sigma_{imp, K_n}}{K_n})^\gamma)} \cdot \frac{\pi}{2}\right)|0\rangle + \sin\left(\frac{1}{1 + \exp(-(\frac{\sigma_{imp, K_n}}{K_n})^\gamma)} \cdot \frac{\pi}{2}\right)|1\rangle.$$

The principle here is that the sigmoid function is used to convert market data to numbers between 0 and 1, and to fuse them into Bloch sphere representations. In the above, F is underlying and β, γ are fixed parameters. For simplicity we consider a fixed maturity and we can extend it to estimating volatility surfaces by putting $\sigma_{imp, K_n} \sqrt{\tau}$ as did in Ruf and Wang (2020) instead of σ_{imp, K_n} , where τ is the time-to-maturity.

The output is then given as the density matrix $\rho_n^{out} = |\phi_n^{out}\rangle\langle\phi_n^{out}|$ and so we need to convert the output to implied volatilities. For example, for the (1,1) element, X , of matrix ρ_n^{out} , we have

$$(3.3) \quad \sigma_{imp, K_n}^{out} = K_n \left(-\log\left(\frac{\pi}{2 \arccos(\sqrt{X})} - 1\right) \right)^{\frac{1}{\gamma}}.$$

4. NUMERICAL EXAMPLES

As numerical examples, we use market data taken from Antonov et al. (2015) and publicly available MATLAB code ¹ provided by Beer et al. (2020). The network consists of one input neuron, one output neuron, and one hidden layer with two neurons ($L=1, m_1 = 2$). The seeds for generating random initial states of $U_j^l(0)$ are set as 0. The learning rate λ is set as 1, ϵ is set as 0.1, and the number of iterations is set as 800. Tables 1 to 3 summarize the comparison results for the output and the training data with different β and γ , while Figure 1 shows plots of these results. Figure 2 and Table 4 show the results for $L = 1, m_1 = 3$, and a slight improvement in the performance can be seen in this case. However, generally, increasing the number of perceptrons in a hidden layer does not result in a substantial improvement. The main reason for this is that this simple numerical experiment only uses one input layer and one output layer. Therefore, a complex network is not required for learning. Additionally, in the present example, an arbitrage-free condition, which the implied volatility surface must satisfy, is not taken into account. A modification such as those in Ackerer et al. (2019) and Itkin (2020) to add constraints that express the arbitrage-free condition in the cost function can be explored. But the modification requires Greeks estimation as well and this motivates us to consider applying DQNN to differential machine learning.

5. DIFFERENTIAL MACHINE LEARNING AS AN APPLICATION TO FINANCE

A second application of the DQNN is for use in differential machine learning (DML), as proposed by Huge and Savine (2020). DML has received great attention in the financial industry. Suppose V is the value of a financial instrument and x is a variable that affects V , such as the interest rate or maturity. The estimation of not only the asset value V , but also the differential $\frac{dV}{dx}$, is important for risk management. DML estimates V and $\frac{dV}{dx}$ efficiently using a twin network scheme: after using a conventional feedforward neural network for predicting V , backpropagation via automatic adjoint differentiation (AAD) is conducted to compute the differential of the output V with respect to the input x . Weights are updated to minimize a cost function consisting of a weighted summation of the prediction errors of V and $\frac{dV}{dx}$. Another upshot of DML is that it can approximate the function of V with respect to x from the shape of the function V via $\frac{dV}{dx}$, which improves the estimation accuracy greatly. Because the idea of the DQNN is analogous to a conventional feedforward neural network, we expect that the implementation of DML in the DQNN will be straightforward, and that the use of the DQNN will improve the efficiency of DML. Given training pairs $\{x_1, V_1\}, \dots, \{x_N, V_N\}$, we consider the following input and output for $n = 1, \dots, N$ and a parameter K

$$|\phi_n^{in}\rangle = \phi_{1,n}^{in}|0\rangle + \phi_{2,n}^{in}|1\rangle, |\phi_n^{out}\rangle = \phi_{1,n}^{out}|0\rangle + \phi_{2,n}^{out}|1\rangle,$$

where

$$\phi_{1,n}^{in} = \cos\left(\frac{1}{1 + \exp\left(-\left(\frac{x_n}{K}\right)^\beta\right)} \cdot \frac{\pi}{2}\right), \phi_{2,n}^{in} = \sin\left(\frac{1}{1 + \exp\left(-\left(\frac{x_n}{K}\right)^\beta\right)} \cdot \frac{\pi}{2}\right)$$

and

$$\phi_{1,n}^{out} = \cos\left(\frac{1}{1 + \exp\left(-\left(\frac{V_n}{K}\right)^\gamma\right)} \cdot \frac{\pi}{2}\right), \phi_{2,n}^{out} = \sin\left(\frac{1}{1 + \exp\left(-\left(\frac{V_n}{K}\right)^\gamma\right)} \cdot \frac{\pi}{2}\right).$$

Let us also assume that $\frac{dV_n}{dx_n}$ is known. Then, in the context of the DQNN, we can apply the twin network proposed in Huge and Savine (2020) to compute the $\frac{d\rho_n^{out}}{dx_n^{in}} = \frac{d\rho_n^{out}}{d\rho_n^{in}} \cdot \frac{d\rho_n^{in}}{dx_n^{in}}$ from the DQNN:

$$\frac{d\rho_n^{out}}{d\rho_n^{in}} \equiv \text{tr}_{in, hid}(\mathcal{U}(I_1 \otimes |0\dots 0\rangle_{hid, out} \langle 0\dots 0|) \mathcal{U}^\dagger),$$

¹The code is available at <https://github.com/qigitphannover/DeepQuantumNeuralNetworks>.

where I_1 is a matrix where every element is equal to one. Also,

$$\frac{d\rho_{n,t}^{in}}{dx_{n,t}^{in}} = \begin{pmatrix} \frac{d(\phi_{1,n}^{in})^2}{dx_{n,t}^{in}} & \frac{d(\phi_{1,n}^{in}\phi_{2,n}^{in})}{dx_{n,t}^{in}} \\ \frac{d(\phi_{1,n}^{in}\phi_{2,n}^{in})}{dx_{n,t}^{in}} & \frac{d(\phi_{2,n}^{in})^2}{dx_{n,t}^{in}} \end{pmatrix} = \begin{pmatrix} 2\phi_{1,n}^{in} \frac{d\phi_{1,n}^{in}}{dx_{n,t}^{in}} & \phi_{1,n}^{in} \frac{d\phi_{2,n}^{in}}{dx_{n,t}^{in}} + \phi_{2,n}^{in} \frac{d\phi_{1,n}^{in}}{dx_{n,t}^{in}} \\ \phi_{1,n}^{in} \frac{d\phi_{2,n}^{in}}{dx_{n,t}^{in}} + \phi_{2,n}^{in} \frac{d\phi_{1,n}^{in}}{dx_{n,t}^{in}} & 2\phi_{2,n}^{in} \frac{d\phi_{2,n}^{in}}{dx_{n,t}^{in}} \end{pmatrix},$$

where

$$\frac{d\phi_{1,n}^{in}}{dx_n} = \frac{\pi}{2} \cdot \frac{\beta}{K} \cdot \left(\frac{x_n}{K}\right)^{\beta-1} \cdot \frac{1}{1 + \exp(-(\frac{x_n}{K})^\beta)} \left[1 - \frac{1}{1 + \exp(-(\frac{x_n}{K})^\beta)}\right] \cdot \sin\left(\frac{1}{1 + \exp(-(\frac{x_n}{K})^\beta)} \cdot \frac{\pi}{2}\right)$$

and

$$\frac{d\phi_{2,n}^{in}}{dx_n} = -\frac{\pi}{2} \cdot \frac{\beta}{K} \cdot \left(\frac{x_n}{K}\right)^{\beta-1} \cdot \frac{1}{1 + \exp(-(\frac{x_n}{K})^\beta)} \left[1 - \frac{1}{1 + \exp(-(\frac{x_n}{K})^\beta)}\right] \cdot \cos\left(\frac{1}{1 + \exp(-(\frac{x_n}{K})^\beta)} \cdot \frac{\pi}{2}\right).$$

On the other hand, we can calculate $\frac{d\rho_{n,t}^{out}}{dx_{n,t}^{out}}$ from the training pair $\{\phi_n^{in}, \phi_n^{out}\}$ as follows:

$$\frac{d\rho_{n,t}^{out}}{dx_{n,t}^{out}} = \begin{pmatrix} \frac{d(\phi_{1,n}^{out})^2}{dx_{n,t}^{out}} & \frac{d(\phi_{1,n}^{out}\phi_{2,n}^{out})}{dx_{n,t}^{out}} \\ \frac{d(\phi_{1,n}^{out}\phi_{2,n}^{out})}{dx_{n,t}^{out}} & \frac{d(\phi_{2,n}^{out})^2}{dx_{n,t}^{out}} \end{pmatrix} = \begin{pmatrix} 2\phi_{1,n}^{out} \frac{d\phi_{1,n}^{out}}{dx_{n,t}^{out}} & \phi_{1,n}^{out} \frac{d\phi_{2,n}^{out}}{dx_{n,t}^{out}} + \phi_{2,n}^{out} \frac{d\phi_{1,n}^{out}}{dx_{n,t}^{out}} \\ \phi_{1,n}^{out} \frac{d\phi_{2,n}^{out}}{dx_{n,t}^{out}} + \phi_{2,n}^{out} \frac{d\phi_{1,n}^{out}}{dx_{n,t}^{out}} & 2\phi_{2,n}^{out} \frac{d\phi_{2,n}^{out}}{dx_{n,t}^{out}} \end{pmatrix},$$

where

$$\frac{d\phi_{1,n}^{out}}{dx_n} = \frac{\pi}{2} \cdot \frac{\gamma}{K} \frac{dV_n}{dx_n} \left(\frac{V_n}{K}\right)^{\gamma-1} \cdot \frac{1}{1 + \exp(-(\frac{V_n}{K})^\gamma)} \left[1 - \frac{1}{1 + \exp(-(\frac{V_n}{K})^\gamma)}\right] \cdot \sin\left(\frac{1}{1 + \exp(-(\frac{V_n}{K})^\gamma)} \cdot \frac{\pi}{2}\right)$$

and

$$\frac{d\phi_{2,n}^{out}}{dx_n} = -\frac{\pi}{2} \cdot \frac{\gamma}{K} \frac{dV_n}{dx_n} \left(\frac{V_n}{K}\right)^{\gamma-1} \cdot \frac{1}{1 + \exp(-(\frac{V_n}{K})^\gamma)} \left[1 - \frac{1}{1 + \exp(-(\frac{V_n}{K})^\gamma)}\right] \cdot \cos\left(\frac{1}{1 + \exp(-(\frac{V_n}{K})^\gamma)} \cdot \frac{\pi}{2}\right).$$

Then, the following cost function is maximized:

$$C_d \equiv \frac{1}{N} \sum_{n=1}^N \langle \phi_n^{out} | \rho_n^{out} | \phi_n^{out} \rangle + \nu \frac{1}{N} \sum_{n=1}^N \mathcal{F}\left(\frac{d\rho_n^{out}}{dx_{n,t}^{out}} \cdot \frac{d\rho_n^{in}}{dx_{n,t}^{in}}, \frac{d\rho_{n,t}^{out}}{dx_{n,t}^{out}}\right),$$

where \mathcal{F} represents fidelity and ν controls the relative influence of the differential constraint to the cost function. The following relationship holds for the two-dimensional matrices A and B (Jozsa (1994)):

$$\mathcal{F}(A, B) = \text{tr}(AB) + 2\sqrt{\det(A)\det(B)}.$$

Then, for the two-dimensional matrices A , B and D , it is straightforward to derive $\mathcal{F}(AD, B) = \mathcal{F}(A, DB)$. Therefore we maximize

$$C_d \equiv \frac{1}{N} \sum_{n=1}^N \langle \phi_n^{out} | \rho_n^{out} | \phi_n^{out} \rangle + \nu \frac{1}{N} \sum_{n=1}^N \text{tr}\left(\sqrt{\left(\frac{d\rho_n^{in}}{dx_{n,t}^{in}} \cdot \frac{d\rho_{n,t}^{out}}{dx_{n,t}^{out}}\right)^{\frac{1}{2}} \frac{d\rho_n^{out}}{dx_{n,t}^{out}} \left(\frac{d\rho_n^{in}}{dx_{n,t}^{in}} \cdot \frac{d\rho_{n,t}^{out}}{dx_{n,t}^{out}}\right)^{\frac{1}{2}}}\right)$$

with which we can apply the original parameter estimation easily. The unitary layers are updated as

$$U \rightarrow e^{iK_d \epsilon} U,$$

where K_d represents the parameterized matrix that is chosen such that C_d increases the most rapidly. A similar argument in the supplementary information of Beer et al. (2020) gives the elements of K_d as follows:

$$K_{d,j}^l = \eta \frac{2^{m_l-1}}{N} \left(\sum_{n=1}^N \text{tr}_{rest} M_j^l + \nu \sum_{n=1}^N \text{tr}_{rest} M_{d,j}^l \right),$$

where

$$M_{d,j}^l = \left[\prod_{\alpha=j}^1 U_\alpha^l (\rho_n^{l-1} \otimes |0\dots 0\rangle_{hidden,out} \langle 0\dots 0|) \prod_{\alpha=1}^j U_\alpha^{l\dagger}, \prod_{\alpha=j+1}^{m_l} U_\alpha^{l\dagger} (\mathbb{I}_{l-1} \otimes \sigma_n^l) \prod_{\alpha=m_l}^{j+1} U_\alpha^l \right]$$

and $\rho_n^l = \varepsilon^l(\dots(\varepsilon^2(\varepsilon^1(I_1))\dots))$, $\sigma_n^l = \mathcal{F}^{l+1}(\dots\mathcal{F}^{out}(\frac{d\rho_n^{in}}{dx_{n,t}^{in}} \cdot \frac{d\rho_{n,t}^{out}}{dx_{n,t}^{out}})\dots)$. Finally, we can extract the predicted V from ρ^{out} and the predicted $\frac{dV}{dx}$ from $\frac{d\rho^{out}}{dx_{n,t}^{out}}$.

6. NUMERICAL EXAMPLES

We use seven training sets of spot price $S(=x)$, call price ($=V$) and delta $\frac{dV}{dS}$ ($=\frac{dV}{dx}$) under the Black–Scholes model with strike $K = 100$, $r = 0.0$, $T = 0.25$, volatility = 0.15. The network consists of one input neuron, one output neuron, and one hidden layer with three neurons ($L=1$, $m_1 = 3$). Tables 5 summarize the comparison results for the output and the training data with different spot prices S . As ν increases, the output of delta gets closer to the training delta, but the price difference also becomes larger. Therefore, careful choice of ν seems to be required.

7. CONCLUSION

The possibility of applying the DQNN proposed by Beer et al. (2020) to finance is investigated. Application to learning implied volatilities with fixed maturity and differential machine learning is explored and these simple numerical results demonstrate that the DQNN is considered to be a promising candidate for developing highly powerful methods in finance. As the next step, further careful investigation will be carried out for practical use such as estimation of the volatility surface and XVA valuation.

REFERENCES

- [1] Akerer, D., Natasa, T., Thibault, V. (2019). Deep smoothing of the implied volatility surface. arXiv: 1906.05065.
- [2] Antonov, A., Konikov, M., Spector, M. (2015). The free boundary SABR: natural extension to negative rates. *Risk*, September.
- [3] Beer, K., Bondarenko, D., Farrelly, T., Osborne, J.T., Salzman, R., Scheiermann, D., Wolf, R. (2020). Training deep quantum neural networks. *Nature Communications*, **11**, 808.
- [4] Brassard, G., Hoyer, P., Mosca, M., Tapp, A. (2002). Quantum amplitude amplification and estimation. *AMS Contemporary Mathematics*, **305**,53-74.
- [5] Fontanela, F., Jacquier, J.A., Oumgari, M. (2019). A Quantum algorithm for linear PDEs arising in Finance. arXiv: 1912.02753.
- [6] Gnoatto, A., Picarelli, A., Reisinger, C. (2020). Deep xVA solver – A neural network based counterparty credit risk management framework. arXiv:2005.02633.
- [7] Hüge, B., Savine, A. (2020) Differential Machine Learning. arXiv:2005.02347.
- [8] Itkin, A. (2020). Deep learning calibration of option pricing models: some pitfalls and solutions. *Risk*, April.
- [9] Jozsa, R. (1994). Fidelity for Mixed Quantum States. *Journal of Modern Optics*, **41**, 2315-2323.
- [10] McClean, J.R., Boixo, S., Smelyanskiy, V.N., Babbush, R., Neven, H. (2018). Barren plateaus in quantum neural network training landscapes. *Nature Communications*, **9**, 4812.
- [11] Ramos-Calderer, S., Pérez-Salinas, A., García-Martín, D., Bravo-Prieto, C., Cortada, J., Planagumà, J., Latorre, J.I. (2019). Quantum unary approach to option pricing. arXiv:1912.01618.
- [12] Ruf, J., Wang, W. (2020). Hedging with neural networks. SSRN 3580132.
- [13] Woerner, S., Egger, D.J. (2019). Quantum risk analysis. *npj Quantum Information*, **5**(15).

| Strike(%) | Training σ (bps) | Output | Diff |
|-----------|-------------------------|--------|------|
| 0.06 | 23.5 | 17.2 | 6.3 |
| 0.31 | 44.7 | 53.5 | -8.8 |
| 0.56 | 59.3 | 62.6 | -3.3 |
| 0.81 | 71.7 | 71.0 | 0.7 |
| 1.06 | 83.0 | 79.7 | 3.3 |
| 1.56 | 103.5 | 97.6 | 5.9 |
| 2.56 | 140.5 | 134.2 | 6.2 |

Table 1. $F = 0.56\%$, $\beta = 1.0$, $\gamma = 1.0$, $C = 0.9984$

| Strike(%) | Training σ (bps) | Output | Diff |
|-----------|-------------------------|--------|------|
| 0.06 | 23.5 | 21.9 | 1.6 |
| 0.31 | 44.7 | 48.3 | -3.6 |
| 0.56 | 59.3 | 61.3 | -2.0 |
| 0.81 | 71.7 | 72.2 | -0.5 |
| 1.06 | 83.0 | 82.2 | 0.8 |
| 1.56 | 103.5 | 100.7 | 2.8 |
| 2.56 | 140.5 | 134.7 | 5.7 |

Table 2. $F = 0.56\%$, $\beta = 0.5$, $\gamma = 0.5$, $C = 0.9998$

| Strike(%) | Training σ (bps) | Output | Diff |
|-----------|-------------------------|--------|------|
| 0.06 | 23.5 | 21.4 | 2.1 |
| 0.31 | 44.7 | 46.7 | -2.0 |
| 0.56 | 59.3 | 61.5 | -2.2 |
| 0.81 | 71.7 | 73.4 | -1.7 |
| 1.06 | 83.0 | 83.8 | -0.8 |
| 1.56 | 103.5 | 101.9 | 1.6 |
| 2.56 | 140.5 | 132.6 | 7.8 |

Table 3. $F = 0.56\%$, $\beta = 0.25$, $\gamma = 0.25$, $C = 0.9997$

| Strike(%) | Training σ (bps) | Output | Diff |
|-----------|-------------------------|--------|------|
| 0.06 | 23.5 | 21.1 | 2.4 |
| 0.31 | 44.7 | 46.1 | -1.4 |
| 0.56 | 59.3 | 61.4 | -2.1 |
| 0.81 | 71.7 | 73.8 | -2.1 |
| 1.06 | 83.0 | 84.8 | -1.8 |
| 1.56 | 103.5 | 104.2 | -0.7 |
| 2.56 | 140.5 | 137.5 | 2.9 |

Table 4. $F = 0.56\%$, $\beta = 0.25$, $\gamma = 0.25$, $m_1 = 3$, $C = 0.9999$

| S | Training price | $\nu = 0.0$ | $\nu = 0.1$ | $\nu = 0.5$ |
|-----|----------------|-------------|-------------|-------------|
| 93 | 0.640 | 0.689 | 0.963 | 1.918 |
| 95 | 1.073 | 1.141 | 1.478 | 2.029 |
| 97 | 1.686 | 1.748 | 2.152 | 2.169 |
| 100 | 2.991 | 2.990 | 3.506 | 2.441 |
| 103 | 4.769 | 4.665 | 5.315 | 2.798 |
| 105 | 6.193 | 6.024 | 6.782 | 3.089 |
| 107 | 7.776 | 7.563 | 8.445 | 3.424 |

| S | Training delta | $\nu = 0.0$ | $\nu = 0.1$ | $\nu = 0.5$ |
|-----|----------------|-------------|-------------|-------------|
| 93 | 0.176 | 0.192 | 0.189 | 0.166 |
| 95 | 0.259 | 0.283 | 0.279 | 0.247 |
| 97 | 0.356 | 0.391 | 0.386 | 0.343 |
| 100 | 0.515 | 0.567 | 0.561 | 0.503 |
| 103 | 0.667 | 0.735 | 0.727 | 0.659 |
| 105 | 0.754 | 0.829 | 0.821 | 0.750 |
| 107 | 0.826 | 0.904 | 0.895 | 0.824 |

Table 5. $\beta = 5.0, \gamma = 0.5$

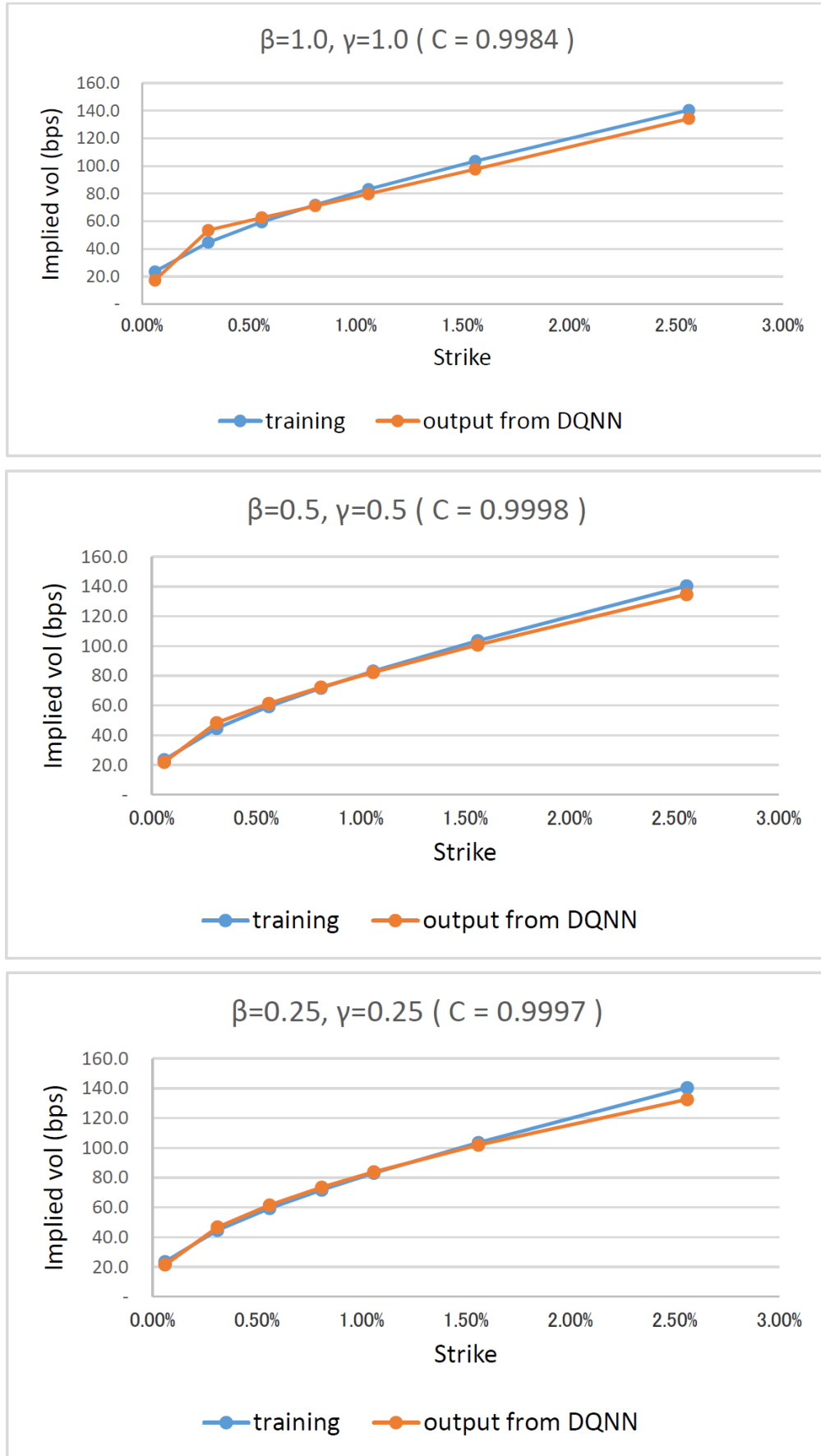


Figure 1. DQNN performance for learning implied volatilities.

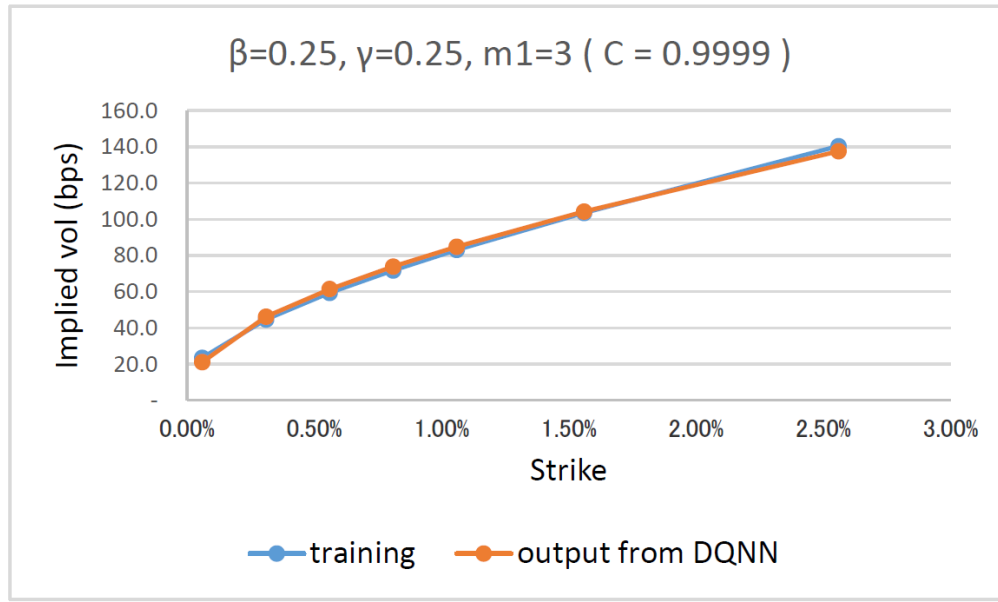


Figure 2. DQNN performance for learning implied volatilities, with $m_1 = 3$.